OPEN ACCESS
Journal of Innovative Optical Health Sciences
2130005 (18 pages)

DOI: 10.1142/S1793545821300056

In vivo imaging and tracking of exosomes for theranostics

Ning Ma*, Changfeng Wu† and Zihui Meng*,‡
*Department of Hepatobiliary-Pancreatic Surgery
China-Japan Union Hospital of Jilin University
Changchun, Jilin 130000, P. R. China
†Department of Biomedical Engineering
Southern University of Science and Technology
Shenzhen, Guangdong 518055, P. R. China
‡zhmeng@jlu.edu.cn

Received 14 June 2021
Accepted 6 August 2021
Published 10 September 2021

Exosomes are lipid bilayer vesicles released by cells and serve as natural carriers for cell–cell communication. Exosomes provide a promising approach to the diagnosis and treatment of diseases and are considered as an alternative to cell therapy. However, one main restriction in their clinical application is that the current understanding of these vesicles, especially their *in vivo* behaviors and distributions, remains inadequate. Here, we reviewed the current and emerging methods for *in vivo* imaging and tracking of exosomes, including fluorescence imaging, bioluminescence imaging, nuclear imaging, X-ray imaging, magnetic resonance imaging, photoacoustic imaging, and multimodal imaging. *In vivo* imaging and tracking of exosomes by these methods can help researchers further understand their uptake mechanism, biodistribution, migration, function, and therapeutic performance. The pioneering studies in this field can elucidate many unknown exosomal behaviors at different levels. We discussed the advantages and limitations of each labeling and imaging strategy. The advances in labeling and *in vivo* imaging will expand our understanding of exosomes and promote their clinical application. We finally provide a perspective and discuss several important issues that need to be explored in future research. This review highlights the values of efficient, sensitive, and biocompatible exosome labeling and imaging techniques in disease theranostics.

Keywords: Exosomes; labeling; tracking; *in vivo* imaging.

‡Corresponding author.

1. Introduction

Extracellular vesicles (EVs) are membranous vesicles secreted by almost all cells.[1] They are rich in proteins, DNAs, RNAs, lipids, and other active ingredients and widely exist in various body fluids, including plasma, lymph, interstitial fluid, cerebrospinal fluid, urine, saliva, milk, etc.[2] According to different formation mechanisms and particle size distribution, EVs are artificially divided into three subgroups: Exosomes (Exos), microvesicles, and apoptotic bodies.[3] Exos are usually defined as EVs less than 200 nm in diameter.[4] Initially, Exos were considered waste products of cell metabolism and received little attention. It was not until 2007 that Valadi *et al.* subversively discovered that mRNA and microRNA in Exos could be transferred to another cell and serve a corresponding regulatory function; this finding changed researchers' perception of Exos.[5,6] With the development of Exos research, people have realized that Exos are important natural carriers for exchanging their complex components between cells and thus participate in various physiological or pathological processes, including cell proliferation, apoptosis, internal environment regulation, immune response, etc.[7–9] The contents and biological functions of Exos are mainly affected by their parent cell resources and physiological states. Three main pathways are involved in the interaction between exosome and their recipient cells: Direct membrane fusion, endocytosis uptake, and activation of lipid ligand receptors.[10,11]

Thus far, exosome-based disease diagnosis and treatment, drug delivery, gene regulation, and other applications have shown satisfying results. Among these applications, Exos secreted by mesenchymal stem cells (MSC-Exos) are considered to be useful for noncellular supportive therapy, since they have been shown to perform bio-functions similar to those of their parent cells. Exos can promote tissue repair and regeneration, enhance cell proliferation, resist inflammatory response, regulate immune response and improve oxidative stress.[12–17] Stem cell transplantation may lead to iatrogenic tumorigenesis, immune rejection, cytotoxicity, tissue and organ embolism and other complications that currently cannot be completely resolved. In contrast, the above problems may be avoided with Exos, due to their advantages of small size, low immunogenicity, low tumorigenicity, and easy preservation, making them a potential alternative to cell therapy. Many studies have confirmed the positive effects of Exos in the treatment of various diseases, including acute and chronic liver injury,[18,19] myocardial infarction,[20] graft-versus-host disease,[21,22] kidney injury,[23] bone or cartilage disease,[24] etc. Exos have good biocompatibility and come from a wide range of sources. They can pass through various biological barriers such as the blood–brain barrier and are ideal carriers for nanodrug or gene delivery engineering. In addition, researchers are working to construct an anti-tumor drug delivery carrier system by using Exos to more precisely target and kill tumors.[25–27]

As a potential noncellular treatment, Exos have shown positive results in disease diagnosis and treatment. The improved symptomology has fully confirmed the effects of Exos in promoting tissue repair, anti-inflammatory, anti-oxidative stress, etc. Nevertheless, the intrinsic mechanisms remain to be further explained. How do Exos perform their biological functions? How do they deliver their content? Which cells are they ingested by? How are they distributed throughout the body? Are there target cells or organs? Will different pathological environments affect their final distribution? Based on the above questions, it is necessary to develop a reliable, noninvasive, and stable exosome imaging technique to reveal their various *in vivo* activities, which will be helpful for further understanding of these extracellular vesicles. This review summarized the current and emerging methods for *in vivo* imaging and tracking of Exos, including fluorescence imaging, bioluminescence imaging, nuclear imaging, X-ray imaging, magnetic resonance imaging, photoacoustic imaging, and multimodal imaging. These methods can help to expand our understanding in the exosome uptake, biodistributions, migration, function, and the final therapeutic performance.

2. Exosome Labeling and *In Vivo* Imaging

In recent years, researchers have constantly proposed the need to "light up" and really "see" extracellular vesicles, so as to develop the imaging and visualization research of tracking EVs at different levels.[28] However, there are many challenges to the visualization research. Exos are extremely small in size but have similar membrane structures to cells.

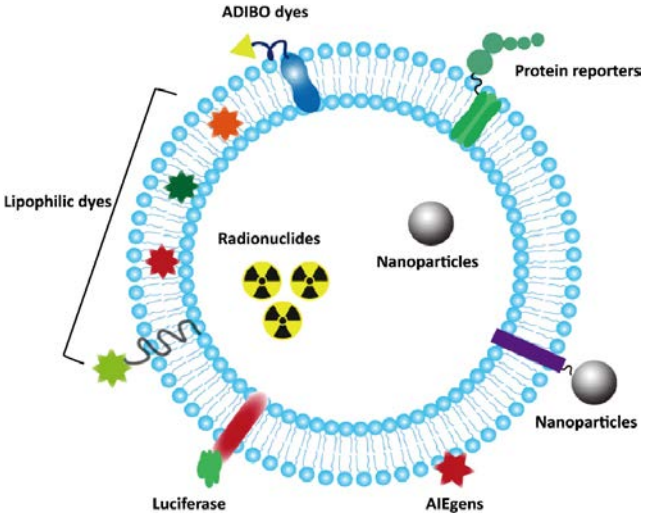

Fig. 1. Different strategies for exosome labeling.

They can rapidly disperse in body fluids. These characteristics necessitate strict requirements for the resolution and contrast of imaging technology.[29] Moreover, the natural membrane barrier of Exos makes it difficult to load imaging agents or drugs. At present, different strategies have been developed for labeling Exos. Commonly used labeling materials include fluorescent dyes, fluorescent proteins, luciferase, radioisotopes, and different nanoparticles such as superparamagnetic iron oxide nanoparticles (SPIOs), gold nanoparticles (GNPs), quantum dots (Qdots), aggregation-induced emission luminogens (AIEgens) (Fig. 1). Most studies have focused on directly or indirectly labeling their parent cells *in vitro*, then transferring them into the body and visualizing them through different imaging modalities. Each labeling method has its advantages and limitations in terms of operation, labeling efficiency, signal strength, toxicity, half-life, etc. When selecting a labeling method, one should choose the appropriate labeling materials according to the experimental direction and emphasis, and the results should be verified and explained in detail. Reported exosome imaging technologies mainly include fluorescence imaging (FLI), bioluminescence imaging (BLI), nuclear imaging, X-ray imaging, magnetic resonance imaging (MRI), and photoacoustic imaging (PAI).[30,31] Fluorescence and bioluminescence imaging are also referred as optical imaging (Table 1).

Table 1. Exosome tracking and imaging techniques.

Technique	Modality	Agent	Source	Route	Time	Ref.
Optical	IVIS	DiD	BM-MSCs	I.V.	6, 24 h	33
	IVIS	DiD	E0771 4T1 67NR	I.V.	4, 24, 48 h	34
	IVIS	DiR	hUC-MSCs	I.V.	3, 6 h	9
	IVIS	DiR	BM-MSCs	I.P.	6, 24, 48 h	35
	CM	PKH26	BM-MSCs	I.V.	8, 16 h	36
	CM	PKH26	BM-MSCs	I.V.	8, 16 h	37
	IVIS	Cy7	MCF-7 MDAMB-231 HS578T	I.V.	24 h	39
	IVIS	Cy5	SKOV3 HEK293	I.V.	24 h	40
	CM	Cy5	MCF-10A MCF-7	I.V.	6 h	41
	CLS	AIEgens	hUC-MSCs	I.V.	1 h 1, 3, 5, 7, 12 d	42
	FM	CFP	MDAMB-231	—	Sustainable	43
	CM	GFP	MMT-060562	—	10 d	44
	CM/MM	PalmGFP	MDAMB-231 EL4	Intratumoral	5 w 9 d	45
	IVIS	eGFP	Milk	I.V.	2, 12 h	46
	IVIS	GLuc-LA	B16BL6	I.V.	10, 30 min 1, 4 h	48, 49

Table 1. (*Continued*)

Technique	Modality	Agent	Source	Route	Time	Ref.
	IVIS	GLuc-LA	B16BL6 C2C12 NIH3T3 MAECs RAW264.7	I.V.	5 min	50
	IVIS	GLuc-LA	hp-MSCs	I.M.	0, 6 h 1, 2, 3 d	51
	IVIS	GlucB	HEK-293T	I.V.	30 min	52
	CM/MM	Fluc	GL261	—	Every 5 min (30 min)	53
	IVIS	Nluc	HT29 HCT116	—	7th w	54
	IVIS	Rluc	CAL-62 MDAMB-231	I.V.	10, 30 min 1, 2, 3, 6, 9 d	55
Nuclear	SPECT/CT	^{131}I	4T1 AT3	I.V.	3, 24, 48 h	57
	γ-Counter	^{125}I	B16BL6	I.V.	1, 5, 10, 30 min 1,4 h	58
	CRC dose calibrator	^{111}In	4T1 MCF-7 PC3	I.V.	24 h	59
	SPECT/CT	^{111}In	B16BL6	I.V.	1, 4, 24 h	60
	SPECT/CT	^{99m}Tc	RAW264.7	I.V.	30 min 1, 3, 5 h	61
	SPECT/CT	^{9m}Tc	RBCs	I.V.	1 h	62
	γ-Camera	^{99m}Tc	RBCs	I.V.	1, 3 h	63
	SPECT/CT	^{99m}Tc	Milk	I.V.	5, 10, 30, 60 min	64
	γ-Counter	^{99m}Tc	HEK-293T	I.V.	1, 2, 4 h	65
	PET	Cu-64	4T1	I.V.	1, 4, 24 h	66
	PET	Cu64 Ca88	4T1	I.V.	24 h	67
	PET	^{124}I	MLP29	I.V. Hock	30 s, 3, 20, 40 min 7, 24, 48, 72 h	68
Tomography	CT	GNPs	hUC-MSCs	Intranasal I.V.	1, 3, 24 h	69
	Micro-CT	GNPs	hUC-MSCs	Intranasal	24 h	70
	CT	GNPs	hUC-MSCs	Intranasal	1, 3, 24, 96 h	71
	SPECT/CT	GNPs	B16BL6	I.V.	6, 24 h	72
	MRI	SPIONs	B16BL7	Foot pad injection	1, 48 h	73
	MPI	SPIONs	MDAMB-231	I.V.	1 h	74
	MRI	USPIOs	ASCs	I.M.	After injection	75, 76
	MRI	GIONs	4T2	I.V.	12 d	78
	MRI	GdL	hUC-MSCs	I.V.	30, 90 min 24 h	77
	MRI	FTH1-LA	BM-MSCs	I.M.	—	79
Photoacoustic	PAI	Anti–EGFR-GNs	3(-) Breast Cancer	I.V.	4, 24 h	84
	PAI	GQDzyme	RBCs	I.V.	2, 4, 8 h	85
	PAI	E6	MIA-PaCa-2	I.V.	After injection	86
	PAI	Gold nanostars	CT26	I.V.	1, 3, 5 min	87

Notes: CLS: Confocal Laser Scanning; CM: Confocal Microscopy; FM: Fluorescence Microscopy; GFP: Green Fluorescent Protein; GdL: Gadolinium; IVIS: *In Vivo* Imaging System; I.V.: Intravenous; I.M.: Intramuscular; I.P.: Intraperitoneal; MM: Multiphoton Microscopy.

2.1. *Fluorescence imaging*

Fluorescence imaging (FLI) is a widely used analytical research technology in biology, pharmacy, and medicine. In recent years, fluorescence technology has been reported to be used for tracking and imaging of Exos. In fluorescent imaging, Exos are labeled with fluorescent dyes, fluorescent proteins, and other fluorescent materials to emit fluorescent signals under external light excitation.

2.1.1. *Fluorescent dyes*

Fluorescent dyes are the most commonly used materials for exosome labeling, tracking, and imaging. Currently, a variety of commercial dyes for exosomes labeling have been developed, including carbocyanine dyes, PKH dyes, and Azadibenzylcyclooctyne (ADIBO) dyes.

Carbocyanine dyes are lipophile dyes that can be embedded into the membrane of exosomes in a noncovalent manner. After entering the lipid bilayer, they diffuse around, thus marking the entire Exos membrane structure. Commonly used carbocyanine dyes include DiR, DiD, and DiL.[32] It is reported that the DiD-labeled MSC-Exos mainly accumulated in the spleen, tibia, and femur marrow of mice suffering from radiation-induced bone marrow injury.[33] Zheng *et al.* established a liver ischemia-reperfusion injury (IRI) mouse model, then injected DiR-labeled MSC-Exos into mice via peripheral veins. They observed that DiR fluorescence was mainly confined to the IRI liver at 3 h and 6 h after injury.[9] DiD-labeled Exos, from highly metastatic breast cancer cells, showed extensive colonization in the lungs of homogenic mice. They created a specific tumor immunosuppressive microenvironment, which promoted metastasis and colonization of cancer foci in lung tissue (Fig. 2).[34] Mendt *et al.* loaded siRNA targeting oncogenic Kras into MSC-Exos through gene editing to treat pancreatic cancer. The DiR-labeled Exos were then intraperitoneally injected (I.P.) to reveal the biological distribution of Exos in tumor mice and healthy controls. Compared with the liver, spleen, and lungs, Exos accumulated more in both normal pancreas and pancreas tumor tissues.[35] PKH dye molecules are also a type of lipophilic dye. Unlike carbonyl cyanine dyes, they have a long aliphatic tail that can be inserted into the lipid bilayer, exposing the fluorophore to the outer lipid bilayer. Tamura *et al.* reported that after injecting PKH26-labeled MSC-Exos into acute liver injury mice, fluorescent signals were presented in the liver tissue, while in the mice receiving PKH-labeled MSCs, the signals remained in the lungs.[36] Exos, whose surfaces were modified by the pullulan, were labeled with PKH dyes. The *in vivo* study confirmed that the surface modification enhanced the anti-inflammatory effects of Exos, and their specific accumulation in the injured liver.[37] The lipophilic fluorescent probe labeling technology has the characteristics of simple operation, high labeling efficiency, strong signal, long life, etc. However, dye aggregation, exogenous substances, or cell membrane fragments will inevitably cause some nonspecific labeling signals, leading to the deviation of experimental results.[38] In addition, their low penetration depths make it difficult for deep tissue imaging.

Azadibenzylcyclooctyne (ADIBO) fluorescent dyes were also reported as exosomes labels. Zhang *et al.* used DBCO-Cy7 to label Exos. Then they observed the specific biological distribution behaviors of different breast cancer Exos. The fluorescent signals of MDA-MB-231 and HS578T cells-derived Exos were found in the brain, liver, kidneys, and lungs, while Exos from MCF-7 cells were mainly concentrated in the liver and kidneys.[39] Kim *et al.* labeled HEK293 and SKOV3 cells-derived Exos with Cy5. They reported that tumor Exos were more likely to target their autologous tumor tissues. It was also confirmed that Exos containing CRISPR/Cas9 suppressed poly polymerase-1 (PARP-1) expression, thus inducing apoptosis of cancer cells.[40] Yang *et al.* transferred Cy5-labeled siRNA into the Exos mimics (EMs) derived from MCF10A cells via electroporation and observed that siRNA enhanced tumor targeting through EMs-mediated delivery.[41] Recent studies have provided a protocol for labeling MSCs-Exos using aggregation luminescence (AIE). AIE-Exos and AIEgens were injected into mice with induced liver injury via peripheral injection. The biological distributions were observed from 1 h to 7 days. In the AIE-Exo group, more signal clustering and stronger signals were detected in the liver region. However, in the AIEgen group, the fluorescence intensity was also very high throughout the experiment period; therefore, a detailed analysis is necessary when comparing groups (Fig. 3). Meanwhile, the authors verified that the efficiency of this labeling method is

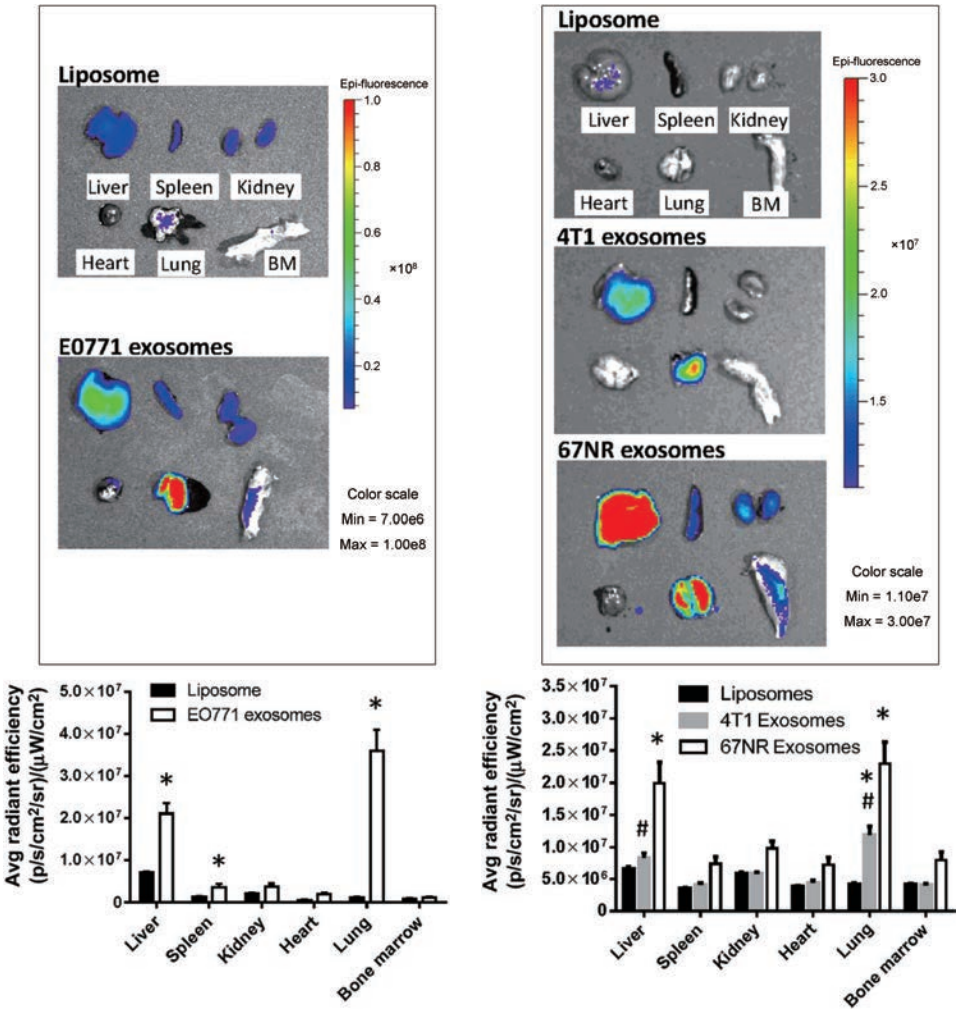

(a) (b)

Fig. 2. *Ex vivo* fluorescent imaging of DiD-labeled Exos derived from (a) E0771, (b) 4T1, and 67NR cells in mice. Exos from all three cell lines accumulated primarily in the lungs. Reproduced with permission from Ref. 34.

better than that of other commonly used fluorescent dyes, including PKH26 and DiL.[42]

2.1.2. *Fluorescent proteins*

Fluorescent proteins, normally known as reporter proteins, emit fluorescent signals under specific wavelengths of excitation light. Fluorescent proteins are fused with molecules on the surface or inside of Exos to construct fusion proteins. Therefore, monitoring the fluorescence signal emitted by the fusion proteins means tracking the labeled Exos.

Zomer *et al.* created MDA-MB-231 cells overexpressing cyan fluorescent protein (CFP) and Cre recombinase (Cre). Exos derived from the above cells contained the Cre-loxp system, which caused the recipient Cre^+ cells presenting DsRed to change color from red to green after receiving Exos. The data reported that Exos released from malignant tumor cells were absorbed by less malignant tumor cells in the same tumor or distant tumor tissue. By receiving RNAs, which were contained in the Exos to regulate metastasis and migration of tumors, less malignant tumor cells showed increased migration behavior and metastasis ability.[43] Suetsugu *et al.* developed GFP-CD63 Exos to analyze their trajectories and functions *in vivo*. In the animal experiments, cancer-derived exosomes resided in the tumor microenvironment, indicating that they may contribute to the formation of an ecological niche promoting tumor growth and metastasis.[44] Enhanced green fluorescent protein (eGFP) and tandem dimer Tomato (tdTomato) were fused with a

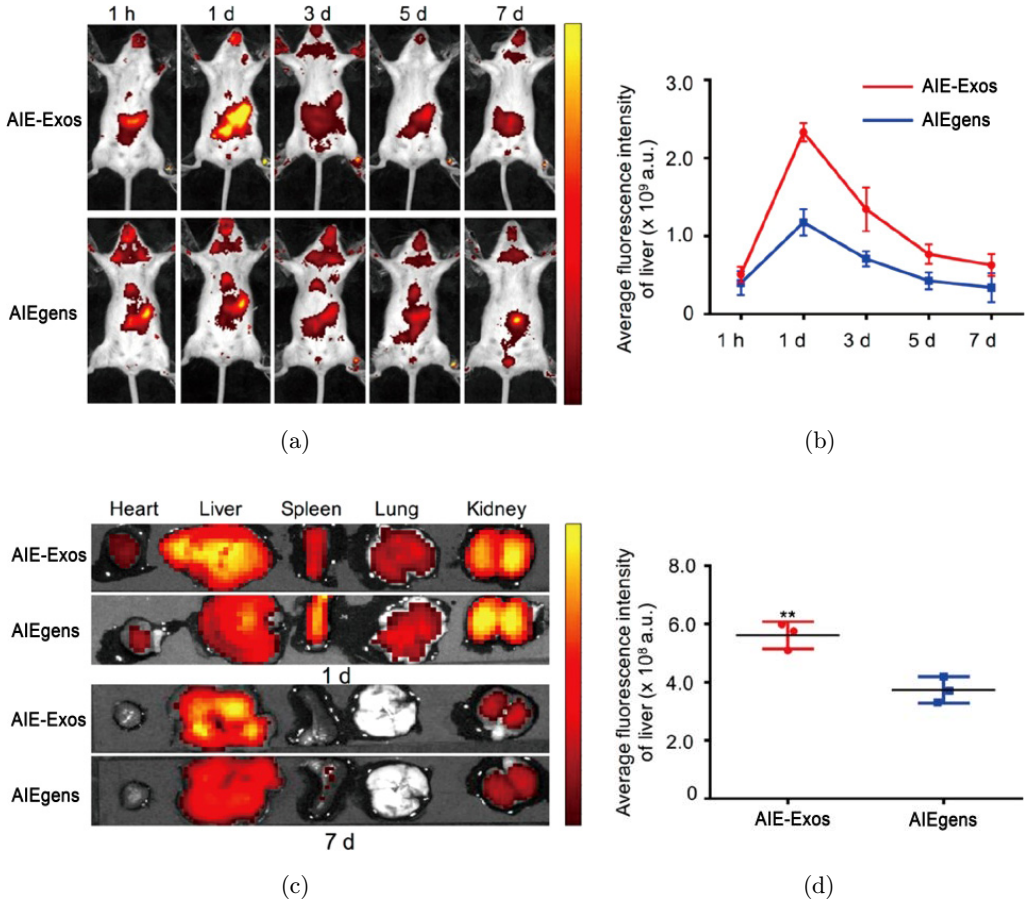

Fig. 3. Exos were labeled and imaged using AIEgens. (a), (b) *In vivo* imaging, the fluorescence signal and intensity of AIE-Exos and AIEgens in acute liver injury mice model. (c), (d) *Ex vivo* imaging, the fluorescence signal and intensity of AIEgens and AIE-Exos in the major organs. Reproduced with permission from Ref. 42.

palmitoylation signal to form a fusion protein (PalmGFP, PalmtdTomato) for exosome membrane labeling. Experiment data confirmed that Exos-mediated intercellular communication was dynamic and multidirectional. This process involved the delivery of functional mRNAs.[45] ZsGreen and eGFP were used to label milk derived Exos. The labeled Exos were mainly concentrated in the liver, spleen, and brain.[46] Fluorescent proteins, which served as reporter genes of various Exos, have high specificity to avoid exogenous fluorescence pollution and fuel aggregation. However, the signal intensity was directly affected by the expression level of fluorescent proteins, membrane labeling efficiency, and excitation light intensity. In addition, whether the fluorescent reporter proteins will affect the membrane structure of Exos as well as their loading and delivery capacity still needs further study and consideration.

2.2. *Bioluminescence imaging*

Bioluminescence imaging (BLI) is another widely used *in vivo* imaging technique. Bioluminescence is a spontaneous bioluminescence phenomenon that occurs when luciferase binds to specific substrates and catalyzes different luminescence reactions. The resulting fluorescence needs no external exciting light but requires an ultra-sensitive camera to capture the instantaneous light signal. The principle of labeling Exos with luciferase is similar to that of the fluorescent protein. Luciferase fuses with exosome-associated proteins. Then the Exos can be tracked by the optical signal produced by luciferase. The difference is that an additional substrate, such as lumen, needs to be injected prior to imaging.[47]

Takahashi *et al.* developed plasmids that express a fusion protein consisting of Gaussia luciferase and a truncated lactadherin (Gluc-LA). B16-BL6 murine melanoma cells were transfected with these

plasmids to secreted Exos (B16-BL6-Exos) labeled with Gluc-LA. *In vivo* pharmacokinetic analysis suggested that Exos remained in circulation for less than 2 min. Serum luciferase activity could barely be detected 4 h after injection, indicating that the B16-BL6-Exos were rapidly cleared in the circulatory system. Additionally, *in vivo* imaging showed that Exos migrated first to the liver, followed by the lungs.[48] They used PKH-labeled B16BL6-Exos to explore this elimination mechanism and demonstrated that these Exos were taken up by macrophages in the liver and spleen and endothelial cells in the lungs. Subsequently, Gluc-labeled B16-BL6-Exos were injected into macrophage-depleted mice and normal controls. The clearance rate of Exos in the experimental group was much lower than that of the normal mice, suggesting that macrophages were mainly responsible for eliminating Exos in the circulatory system (Fig. 4).[49] Charoenviriyakul *et al.* collected Exos from five different mouse cell lines: B16-BL6 mouse melanoma cells, C2C12 mouse myoblast cells, NIH3T3 mouse fibroblasts, MAEC mouse aortic endothelial cells, and RAW264.7 mouse macrophage-like cells. The Exos were labeled with luciferase and lactinin fusion protein to evaluate their pharmacokinetics *in vivo*. The results showed that all Exos delivered intravenously disappeared rapidly from the blood circulation and mainly accumulated in the liver tissue.[50] Zhang *et al.* investigated the bio-distribution of Gluc-labeled MSC-Exos, which were incorporated with chitosan hydrogel (CS-Exos), in the hind limb ischemia mice. BLI data showed that mice in both groups had strong Gluc signals in their hind limbs within 24 h after injection. In contrast to the rapid dissipation of fluorescence signals in the Exo group, Gluc signals could still be obtained in the CS-Exo group 72 h after injection, indicating that CS-Exos could significantly improve the retention rate and stability of MSC-Exos throughout the whole body.[51] Gluc binds to metabolic biochemical receptor peptides to produce a reporter protein (GlucB) for labeling Exos (GlucB-Exos). In the mice models, bioluminescence and

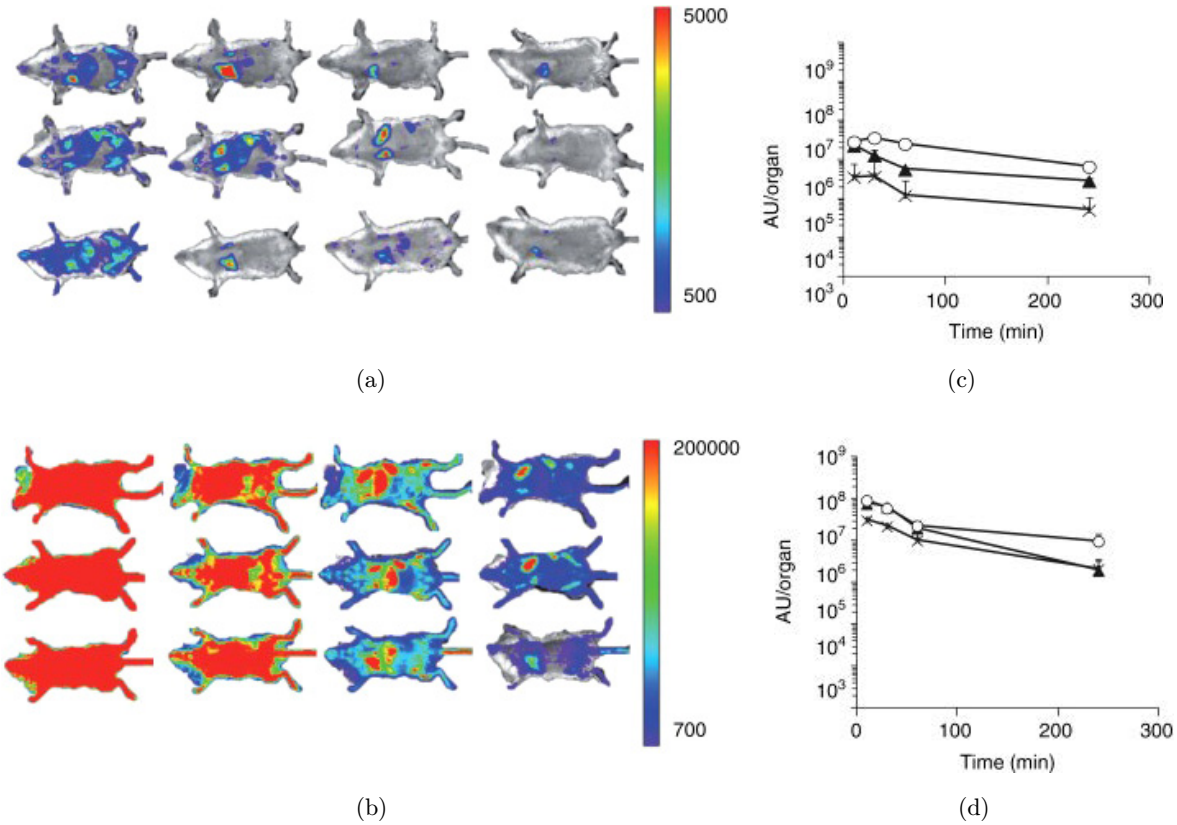

Fig. 4. *In vivo* bio-distribution of B16BL6-Exos. (a), (c) *In vivo* fluorescence imaging signal and chemiluminescence intensity of Gluc-LA-labeled B16BL6-Exos in normal mice. (b), (d) *In vivo* fluorescence imaging signal and chemiluminescence intensity of Gluc-LA-labeled B16BL6-Exos in macrophage-depleted mice. Reproduced with permission from Ref. 49.

fluorescence-mediated laminography showed that Exos were mainly localized in the spleen, followed by the liver. GlucB-Exos were injected into thymic nude mice with human Gli36-mcherry gloma xenograft tumors transplanted subcutaneously to the left and right chest. Exosome signals were located at the tumor site 60 min after administration.[52]

Firefly luciferase (Fluc) was also reported to have tracked Exos and their internal nucleic acid delivery. Van der Vos *et al.* observed the *in vivo* behaviors of glioblastoma cells Exos (GBM-Exos) that express Fluc, mCherry, and palmtd-Tomato proteins, using multiphoton intravital microscopy (MP-IVM). In the *in vitro* experiment, microglia cells actively ingested GBM-Exos, showing a tendency toward hyperproliferation and immunosuppression. Inhibitor nucleic acid miR-451/miR-21 contained in GBM-Exos were transferred to microglia cells, silencing their targeted c-Myc-mRNAs. In the *in vivo* analysis, they observed the release of GBM-Exos and their uptake by microglia and mononuclear/macrophage cells.[53] NanoLuc (Nluc) made it possible to assess and detect Exos uptake by recipient cells or tissues. For *in vivo* imaging, HT29 and HCT116 cells expressing CD63-Nluc, coated with matrigel, were implanted in mice with mCherry markers to distinguish exosome-derived luminescence from cell-derived luminescence. The data showed that the transplanted cells constantly provided Exos to the whole body for seven weeks, and strong luminescence signals were observed in the stomach and intestines.[54] Renilla luciferase (Rluc) is also a reporter protein for labeling Exos (Rluc-Exos). Gangadaran *et al.* created Rluc-Exos to observe the *in vivo* distributions of Exos from different tumor cells. They found that the signals of Cal-62 cells-derived Exos were stronger in the lungs, compared with the liver, while the signals of MDA-MB-231 cells-derived Exos were more concentrated in the liver tissues.[55]

Bioluminescence imaging technology has the advantages of low background signal, high specificity, and reliability. It can avoid the misleading signals caused by dye aggregation. However, luciferase labeling, similar to fluorescent proteins and fluorescent dyes, also has limits such as low labeling efficiency, short half-life, complex parent cell transfection process, and low tissue penetration depth. Moreover, substrates with an extremely short half-life (peaks by 1 min, lasts 5 min at most) need to be injected before each imaging, which requires high time management and equipment precision.

2.3. *Nuclear imaging*

Nuclear imaging is a noninvasive cell imaging technique. A gamma camera or PET/CT equipment is used to collect the radiation signals emitted by radionuclides. The image is formed after computer processing.[56] The researchers were able to track the biodistribution of the Exos by loading or labeling them with radionuclides. Commonly used radionuclides for Exos imaging include ^{131}Iodine (^{131}I), ^{125}I-iodobenzoylde-formamide (^{125}I), ^{111}Indium (^{111}In), and Technetium-99m (^{99m}Tc).

^{131}I-loaded tumor cell-derived Exos (^{131}I-Exos) were injected through a caudal vein into mice with primary tumors and lung metastases. The SPECT/CT scans were performed 3, 24, and 48 h after administration. The primary and metastatic tumor sites of the mice showed sufficient radioactivity 3 h postadministration. In contrast, the tumor-free mice had little radioactivity in the breast fat pads but a large amount of radioactivity in the lungs. Researchers then investigated the biodistributions of Exos from other cell lines in tumor mice. ^{131}I-Exos from all cell lines except HEK293 cells were concentrated in primary breast tumors and lung metastases 3 h after injection. Notably, EPC Exos were heavily distributed at the primary tumor site, while MDSC Exos were more visible in the lungs at metastatic sites than in other groups.[57] Morishita *et al.* labeled B16-BL6 derived Exos with iodine-125 (^{125}I), based on a streptavidin (SAV)-biotin system. After intravenous injection of ^{125}I labeled Exos, radioactive signals dissipated rapidly in the circulation system. At 4 h, the liver tissues showed the highest radioactivity (28%), followed by the lungs (7%) and spleen (1.6%). It can be inferred that the liver is the main organ for clearing exogenous B16-BL6 derived Exos.[58] Smyth *et al.* used ^{111}In-oxine-labeled Exos to explore their biological distribution *in vivo*. Three hours after intravenous administration, the circulatory radioactivity signal decreased by more than 95% of its initial strength. After 24 h, the radiological signals of both PC3 and MCF-7 cells-derived Exos were cleared rapidly from the blood of tumor-bearing mice. Both tumor-bearing and normal mice showed similar trends in Exos

clearance. The bio-distribution analysis of *ex vivo* organs indicated that the accumulation of Exos from both types of cells was higher in the liver, spleen, and kidneys than in other organ tissues.[59] ^{111}In-oxine covalently binds to the vesicle membrane to create Exos labeled with ^{111}In markers (^{111}In-B16F10-Exos). ^{111}In-B16F10-Exos were injected intravenously into tumor-bearing mice. Their *in vivo* distribution in tumor-bearing mice was monitored using whole-body SPECT/CT imaging at 30 min, 4, and 24 h postinjection. The authors observed a significant accumulation of Exos in the liver and spleen, followed by the kidneys, while minor in the tumor tissues (Fig. 5).[60]

Radionuclide ^{99m}Tc-labeled Exos have been used to track and image exosomes. Hwang *et al.* used ^{99m}Tc-HMPAO to radiologically label macrophage-derived exosome mimetic vehicles (EMVs). Then they monitored the distribution of ^{99m}Tc-HMPAO-EMVs *in vivo* via SPECT/CT. Radioactive signals were primarily concentrated in the liver rather than in the brain.[61] The ^{99m}Tc-Tricarbonyl complex, which directly binds to a variety of amino acids that may exist on the exosome membrane, was used to label Exos. The result showed that Exos administered intravenously were mostly concentrated in the liver and spleen.[62] ^{99m}Tc-labeled blood cell-derived exosome mimics (RBC-EMs) were imaged *in vivo* via a gamma camera at 1 and 3 h postinjection. Compared with free ^{99m}Tc, ^{99m}Tc-RBC-EMs accumulated more in the liver and spleen of mice but less in the thyroid. The *in vitro* imaging further confirmed the results *in vivo*.[63] Gonzalez *et al.* injected ^{99m}Tc-labeled milk-derived Exos into mice. Longitudinal tracking showed that these nanotracers could be quickly cleared from the blood. SPECT/CT revealed that radiation signals were visible in the aorta and pulmonary circulation 5 min after injection and began to accumulate in the liver at 10 min. Rapid excretion was confirmed by the high accumulation activity that existed in the bladder at 30 and 60 min. Exos were observed to be mainly distributed in the liver and spleen tissues 1 h postinjection, and no significant changes in their internal locations were found at 3, 5, and 24 h.[64] Molavipordanjani *et al.* used ^{99m}Tc-labeled exosomes (^{99m}Tc-Exos) targeting HER_2 for tumor imaging. The biodistribution analysis indicated the tendency of these ^{99m}Tc-Exos to be localized in tumors. Trastuzumab, which was utilized for blocking the HER_2 receptors, decreased the accumulation of ^{99m}Tc-Exos in tumor tissues.[65] Shi *et al.* reported a successful example of noninvasive monitoring of the copper-64 ((64)Cu)-labeled PEG-modified Exos using PET. The PEG modification conferred superior pharmacokinetic properties onto the Exos, enabling them to accumulate more in tumors. Moreover, such kind of modification also reduced premature liver isolation and exosome clearance. These findings are expected to enhance the delivery efficiency and safety of exosome-based therapy.[66] Subsequently, Jung *et al.* successfully labeled breast cancer Exos with (64)Cu and fluorescence dyes. PET and optical imaging were used to monitor the Exos distribution *in vivo*. Exos entered the sentinel lymph nodes of the drainage via

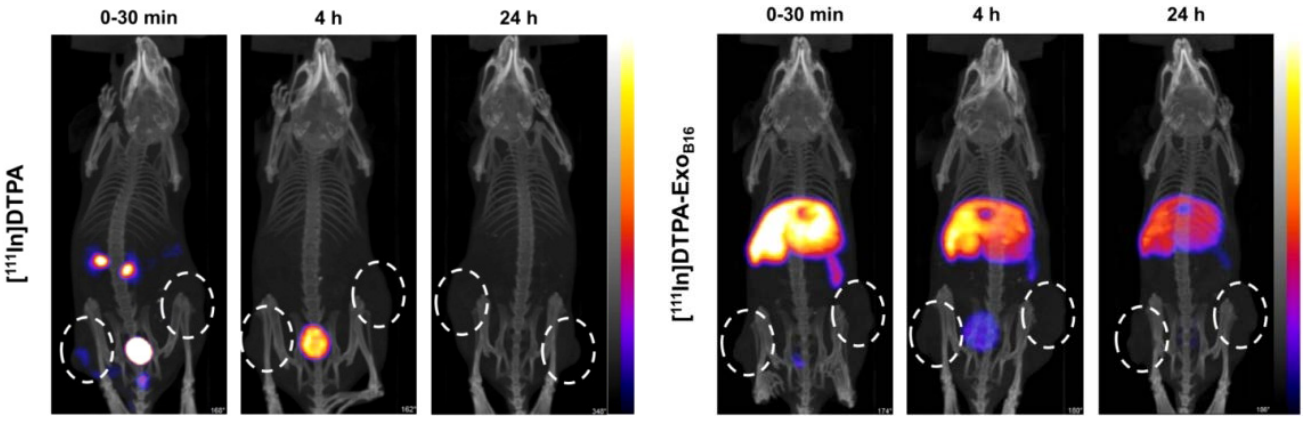

(a) (b)

Fig. 5. SPECT/CT images. *In vivo* bio-distribution of B16F10 derived Exos in melanoma-bearing mice. (a) Free [^{111}In]DTPA were injected as a control. (b) [^{111}In]DTPA-Exos were injected into the mice. The images were obtained 30 min, 4, and 24 h postinjection. White circles indicate the position of tumors. Reproduced with permission from Ref. 60.

the lymphatic injection route, whereas they significantly accumulated in the lungs, liver, and spleen via the blood administration route.[67] Royo *et al.* directly labeled Exos with [124I]NaI and injected them intravenously into mice or joints. *In vivo* radioactivity levels of major organs at different time points were measured with PET. The results suggested that IV injection could lead to a rapid accumulation of Exos in the liver, but this biodistribution changed as visible signals appeared in different organs several hours later.[68]

Radiological labeling provides clear, deeply penetrating, and whole-body imaging of Exos. It also allows for anatomical imaging and three-dimensional localization visualization of Exos. However, the half-lives of most radionuclides are very short, leading to difficulties for long-term *in vivo* tracking. Nuclear imaging technology has a high technical threshold. The imaging process requires a trained professional to handle radioactive molecules. Furthermore, the biomedical use of radioactive molecules is strictly controlled.

2.4. *X-ray imaging*

X-ray imaging is a fast and useful imaging technique that has been developed for tracking and imaging of Exos. Metal nanoparticles are used as tracers to label Exosome. X-ray computed tomography (CT) was used to obtain real-time visualization of Exos *in vivo*.

CT conducts a sequential cross-sectional scan around a certain part of the body using various rays, including X-ray, γ-ray, ultrasonic wave, etc. Highly sensitive detectors receive the radiation passing through, which is processed by a computer to produce an image. CT is one of the most convenient imaging tools in clinical practice due to its fast scanning time and high resolution. In recent years, CT has also been used to detect the biological distribution of Exos *in vivo*. Betzer *et al.* developed glucose-coated gold nanoparticles (Glu-GNPs) to label Exos. Glu-GNPs entered the Exos through the glucose transporter (Glut-1) on the membrane surface, thus achieving the loading of Glu-GNPs by exosome vesicles. Using a CT scan, they found that Exos administered intranasally resulted in a greater accumulation in the brain than those administered intravenously (Fig. 6).[69] Subsequently, the same team used Glu-GNPs to label special MSC-Exos, which were edited to contain phosphatase and tensin homolog siRNA. They investigated the targeting effect of these Exos for spinal cord injury after intranasal injection. The results showed that Exos could target the injured spinal cord through the blood–brain barrier. The siRNAs in these Exos could down-regulate phosphatase and tensin homolog (PTEN) expression in the injured spinal cord.[70] Based on this labeling approach, they further monitor the migration and colonization of intranasally administered MSC-Exos in various brain lesions, including stroke, autism, Parkinson's disease, and Alzheimer's disease. The results showed that MSC-Exos specifically targeted the lesion area of the mouse brain and accumulated for 96 h. However, Exos showed a diffusion migration pattern in the healthy controls. They were cleared from the lesion area after 24 h. Confocal microscopic observation of the lesion area confirmed that MSC-Exos were selectively taken up by neuronal cells rather than glial cells.[71] Lara *et al.* established a new protocol for loading gold nanoparticles (AuNPs) into Exos. B16F10 cells ingested folate (FA)-conjugated AuNPs, and the AuNPs were internalized into the cytoplasm. They were loaded by Exos and subsequently expelled to the extracellular space. The *in vivo* experimental results suggested that B16F10 cells were more likely to absorb Exos of their own origin than those derived from colorectal adenoma, macrophage, and kidneys. B16F10 cells-derived Exos preferentially accumulated in small lung metastases compared to the other organs.[72]

2.5. *Magnetic resonance imaging*

Magnetic resonance imaging (MRI) uses magnetic resonance phenomena to obtain electromagnetic signals from the human body and reconstruct information about the body. It has the advantages of noninvasive radiation, high spatial and soft tissue resolutions. Magnetic labeling of Exos enables *in vivo* tracking and visualization of Exos by using MRI. Currently reported contrast agents to include SPIONs, gadolinium, gold-iron oxide nanoparticles (GIONs), and ferritin heavy chain (FTH1). Initially, Hu *et al.* described the preparation of Exos loaded with 5 nm SPIONs by electroporation. In the *in vivo* experiment, they observed, via MRI, the migration of melanoma Exos from footpads to lymph nodes 48 h after intravenous injection in

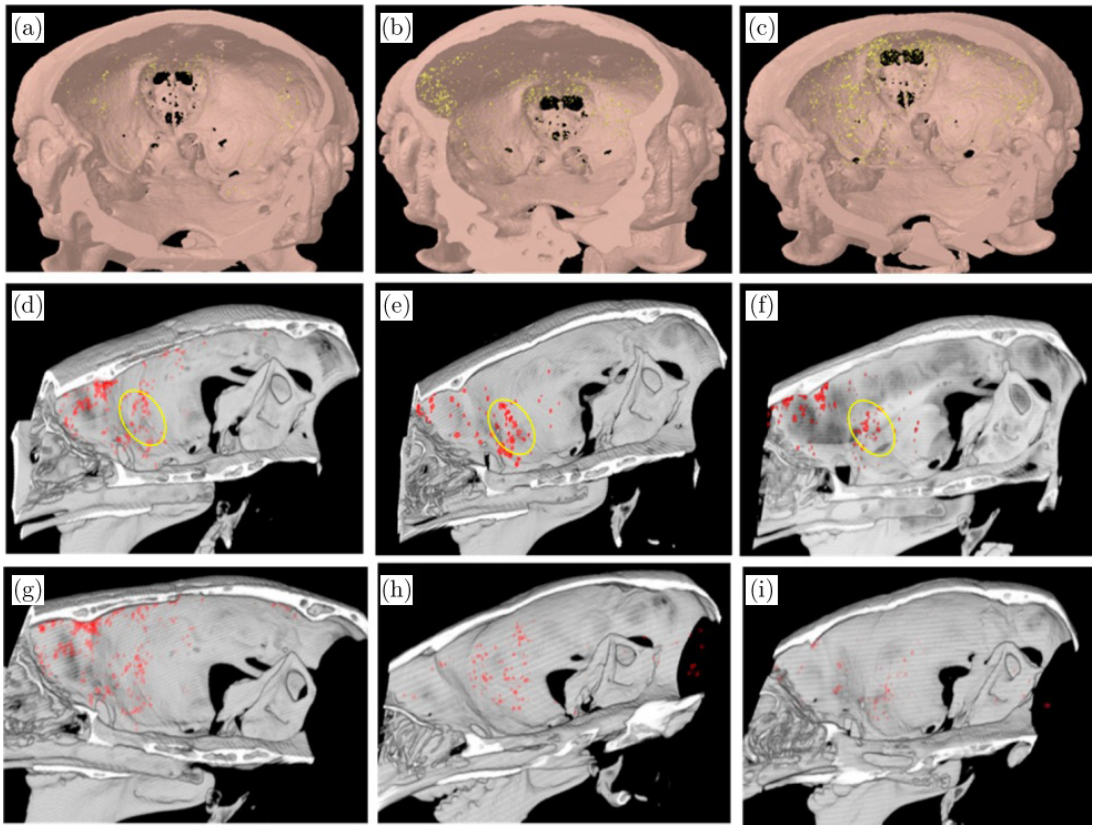

Fig. 6. CT imaging of Glu-GNPs labeled MSC-Exos in mice with acute striatal stroke. (a), (d) (b), (e) (c), (f) represent the 3D body images of the brain at 1, 3, and 24 h after exosome administration, respectively (a yellow circle marked the ischemic area). After 3 h, MSC-Exos migrated to the ischemic area. In contrast, MSC-Exos in the nonischemic control mice (g)–(i) did not accumulate in any region specifically and were cleared from the brain 24 h after administration. Reproduced with permission from Ref. 69.

mice.[73] Jung *et al.* indirectly loaded MD-MB-231 cells with SPIONs to generate Exos that could be tracked by magnetic particle imaging (MPI) *in vivo*. The results confirmed that the Exos were mainly concentrated in the liver 1 h after the injection of SPION-loaded-Exos in healthy mice. Further, the MPI also approved the successful accumulation of Olapari-SPION-loaded Exos in the tumors of MDI-MB-231 xenograft mice, while delaying tumor growth.[74] Busato *et al.* reported a method for labeling Exos with ultrasmall SPIONs (4–6 nm). This protocol retained the original morphology and physiological characteristics of Exos and endowed them with the ability to be imaged under MR.[75,76] In a recent study, gadolinium-labeled MSC Exos (Exos-GDL) were used to investigate their activities in osteosarcoma mice by MRI. Exos were observed to accumulate continuously in tumors at 24–48 h postinjection. In contrast, the synthetic lipid nanoparticles only accumulated in tumors within 3 h after injection.[77] Bose *et al.* fused GIONs with Exos (GION-Exos) through a top–down process (including extrusion of the porous membrane at 100 nm). Those labeled Exos were injected three times into tumor-bearing mice. The MRI revealed a strong GION-Exo signal in tumors at 12 d.[78] Ferritin heavy chain (FTH1) and a truncated lactadherin were engineered to synthesize a fusion protein. FTH1 was regarded as an MRI reporter that allowed the biodistribution of exosomes to be visualized *in vivo*.[79]

With the high spatial resolution and deep tissue penetration, X-ray CT and MRI techniques make it possible to achieve long-term *in vivo* tracking of Exos. It should be taken into consideration that the signal we see only reflects the *in vivo* trajectories of the markers, which indirectly reveals the location information of Exos. Moreover, the labeling materials may not remain in the vesicle throughout the whole process; they may be released at some stage. Therefore, such an approach may not provide the true fate of all Exos, leading to biased results.

2.6. *Photoacoustic imaging*

Photoacoustic imaging (PAI) is a promising biomedical imaging technology that integrates optical imaging and ultrasonic imaging. Under pulsed laser irradiation, tissue or contrast agents receive photothermal expansion and produce an ultrasonic signal.[80,81] PAI is characterized by high spatial resolution, deep penetration depth, and high contrast, which combine the advantages of ultrasonic and optical imaging.[82,83] Piao *et al.* used PAI to monitor tumor growth and axillary lymph node metastasis. Anti-EGFR gold nanoparticles, as PAI contrast agents, specifically bind to $EGFR^+$ Exos. The results confirmed that homologous Exos promote primary tumor growth and axillary lymph node metastasis.[84] Graphene quantum dot nanozyme (GQDzyme), with its intrinsic peroxidase activity, can effectively convert ABTS (3-ethylbenzothiazo-line-6-sulfonic acid) to its oxidation state, $ABTS^+$, in the presence of H_2O_2. The latter has a strong near-infrared (NIR) absorption capacity for PAI. Based on this principle, Ding *et al.* constructed exosome-like nanozyme vesicles derived from red blood cells and observed that these exosomal-like vesicles accumulated in the tumor area 2 h after administration, with the PAI signal increasing up through 8 h.[85] Chlorine e6, as a photosensitizer, loaded in the tumor-derived re-assembled exosomes (R-Exos), made it feasible for visualizing of the Exos via PAI.[86] Recent studies have also reported PAI of Exos based on gold (Au) nanostars. Incubating tumor cells with gold nanostar produced a large amount of tumor cell-derived stellate plasmonic exosomes (TDSP-Exos), which could be seen under PAI. Moreover, these Exos also have a certain therapeutic significance. TDSP-Exos improved tumor hypoxia, enhancing radiotherapy by NIR-II photothermal therapy (Fig. 7).[87] PAI is a noninvasive technique for tracking and imaging Exos in deep tissues as compared to optical methods. With the development of materials science, various tracers with photoacoustic imaging and photothermal therapy dual characteristics have been prepared. Combining of Exos with such tracers may allow for better targeting and damage of tumor cells and visualization of the therapeutic process, which may be a new strategy for tumor therapy in the future.

2.7. *Multimodal bioimaging*

Currently, multimodal bioimaging has become a powerful tool to reveal the behavior of Exos in combination with a variety of imaging techniques. Multiple modes complement each other, thus expanding the application range of the dynamic tracking system and improving the imaging accuracy. Zhao *et al.* achieved *in vivo* bimodal visualization of EVs by synthesizing ultra-small particles,

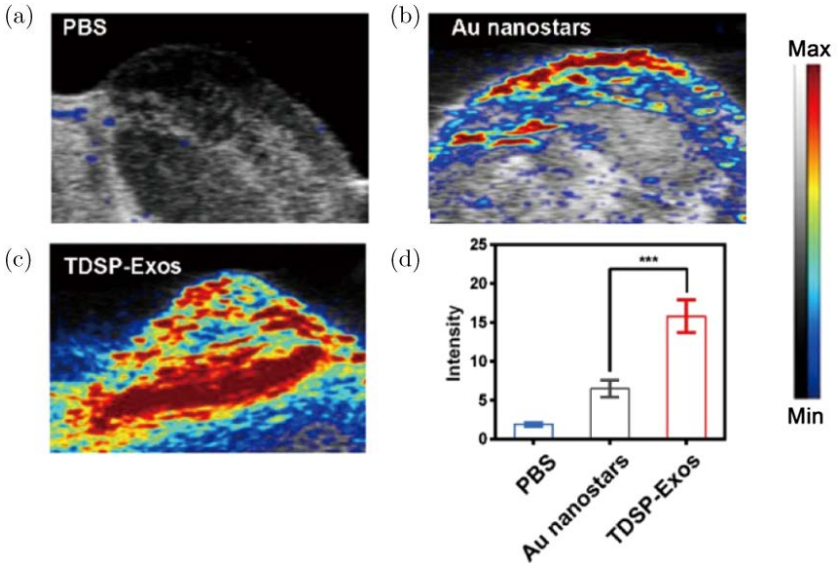

Fig. 7. Representative PA images of murine tumors at 24 h postinjection of (a) PBS, (b) Au nanostars, or (c) TDSP-Exos. (d) TDSP-Exos associated PAI signals were significantly higher in tumors than that of free Au nanostars. Reproduced with permission from Ref. 87.

Quantum Dots (Ag_2Se Quantum Dots), that possess both MRI and near-infrared (NIR) fluorescence bimodal imaging capabilities (Fig. 8).[88] Cao *et al.* engineered exosome-mediated NIR-II region vanadium carbide quantum dots, which were revealed to have FLI, PAI, and MRI capabilities. The resulting nanoparticles proved feasible for the clinical application of NIR-II low-temperature nuclear targeted photothermal therapy.[89] Iridium and iron oxide nanoclusters (NCs), biosynthesized *in situ* by cancer cells or tumor tissues, have been regarded as ideal probes for multimodal imaging. They enhanced the image sensitivity and specificity for tumor tissues.

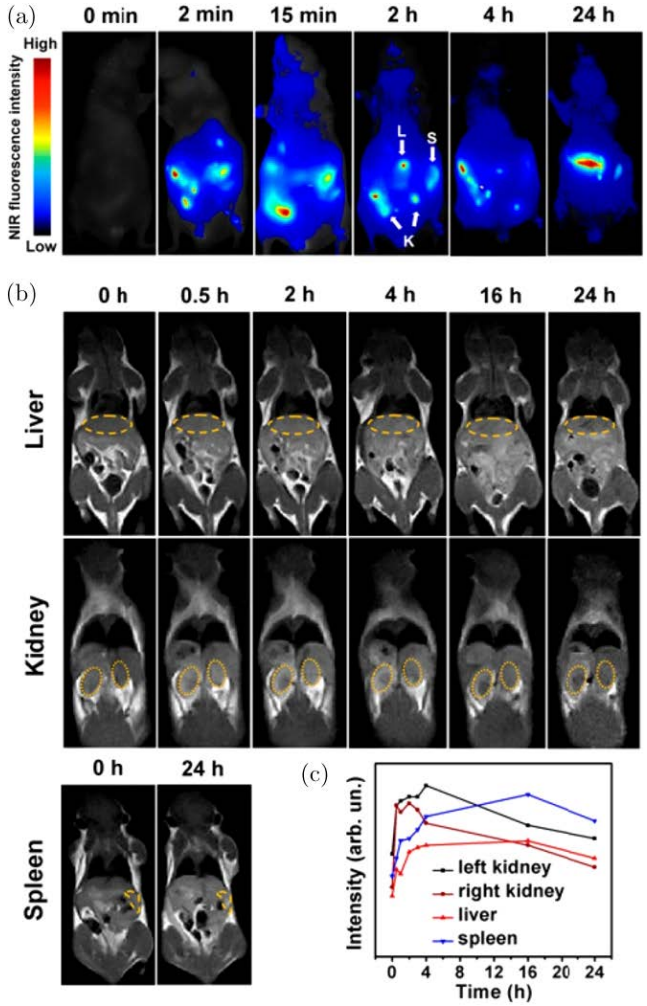

Fig. 8. Fluorescence images and MR images of mice at 0–24 h postinjection of the Ag_2Se Q dots labeled extracellular vesicles. (a) NIR fluorescence images of liver, kidneys, and spleen. (b) T_1-weighted images of liver, kidneys, and spleen. (c) Quantitative analysis of the T_1 signal intensity. Reproduced with permission from Ref. 88.

These NC-loaded tumor cell-derived Exos can also be used as tumor-specific biomarkers.[90]

3. Summary and Outlook

This review summarized the recent advances in *in vivo* imaging and tracking of Exos and described each of their advantages and limitations. Most of these methods are pioneering and can elucidate many unknown *in vivo* behaviors of Exos at different levels, including bio-distributions, migrations, functions, uptake mechanisms, information exchange patterns, etc. Exosome-based tumor diagnosis, drug delivery, and barrier penetration functions have also been further validated. Exos have become the focus of this research due to their inherent ability to transmit biological information and their potential drug delivery ability. To clarify the unclear behaviors and functions of Exos *in vivo* may promote their translation to clinical applications. With the improvement of labeling methods and tracking techniques, the mysteries of Exos are being unveiled.

Despite the promising applications, there still exist several vital aspects that need to be explored in future research. First, there is a lack of standard separation and purification procedures for Exos, which leads to high contamination in the isolation process of samples. For example, lipoprotein can significantly interfere with the staining process of Exos with lipophilic dyes and thus affect the determination of their distribution *in vivo*. In addition, under physiological and pathological conditions, even the same cell line may secrete exosome subpopulations carrying different information and exhibit different distributions and biological functions. Unfortunately, there is currently no method to isolate these exosome subpopulations based on their physical properties and intrinsic composition. Second, the Exos administration dose is not uniform across various literatures. Commonly used dose units include particle number, protein quantification, radiation dose, etc. Therefore, dose standardization is recommended for future studies in order to obtain more measurable comparisons between different studies. In addition, different dose administration methods may also affect the distribution and biological function of Exos *in vivo*. Data obtained from the comprehensive observation of a sequential dose gradient are more convincing.

Third, it should be taken into account that the route and timing of administration may influence the accumulation pattern of Exos *in vivo*. The fundamental goal of exosome research is to explore as many applicable conditions as possible for its future clinical applications. Therefore, in the study of exosome-based disease treatment, researchers should comprehensively explore the results under different administration routes and timing conditions and conduct detailed comparisons and analyses of the data to accumulate more reference basis for clinical application. Fourth, current imaging platforms that are dedicated to the dynamic tracking of Exos are almost lacking. Currently used optical imaging, MRI, and radionuclide imaging platforms all attempt to achieve downward compatibility of Exos by adjusting parameters on the basis of cell tracers or even medical imaging equipment, which inevitably leads to compromising the experimental design based on the instrument threshold. It is urgent to establish a specific dynamic imaging platform for Exos tracking. Fifth, due to the absence of an exosomal-specific imaging platform system, it is necessary to advocate the application of multimodal imaging methods with comprehensive advantages that can reveal the true fate of Exos through multiple confirmations. However, there are only a few reports on multimodal exosome imaging at present.

Exos hold promising prospects. The rapid development of imaging technologies provides a powerful hardware foundation for exploring exosomal activities *in vivo*, including intercellular information exchange, gene regulation, homing and migration, etc. Future research will undoubtedly allow us to have complete knowledge of their capabilities and limitations. With this adequate cognitive guidance, exosome-based therapy can be progressively promoted from the laboratory to the clinic.

Conflict of Interest

The authors declare that there are no conflicts of interest relevant to this article.

Acknowledgments

This study was funded by the Key Scientific and Technological Research and Development Project of Jilin Province (No. 20180201055YY), National Key R&D Program of China (Grant Nos. 2020YFA0909000 and 2018YFB0407200), the Shenzhen Science and Technology Innovation Commission (Grant No. KQTD20170810111314625), and the National Natural Science Foundation of China (Grant No. 81771930).

References

1. E. L. Andaloussi, S. I. Mager, X. O. Breakefield, M. J. Wood, "Extracellular vesicles: Biology and emerging therapeutic opportunities," *Nat. Rev. Drug Discov.* **12**, 347–357 (2013).
2. C. Thery, S. Amigorena, G. Raposo, A. Clayton, "Isolation and characterization of exosomes from cell culture supernatants and biological fluids," *Curr. Protoc. Cell Biol.* **Chapter 3**, Unit 3.22 (2006).
3. J. C. Akers, D. Gonda, R. Kim, B. S. Carter, C. C. Chen, "Biogenesis of extracellular vesicles (EV): Exosomes, microvesicles, retrovirus-like vesicles, and apoptotic bodies," *J. Neurooncol.* **113**, 1–11 (2013).
4. C. Thery *et al.*, "Minimal information for studies of extracellular vesicles 2018 (MISEV2018): A position statement of the international society for extracellular vesicles and update of the MISEV2014 guidelines," *J. Extracell Vesicles.* **7**, 1535750 (2018).
5. R. M. Johnstone, M. Adam, J. R. Hammond, L. Orr, C. Turbide, "Vesicle formation during reticulocyte maturation. Association of plasma membrane activities with released vesicles (exosomes)," *J. Biol Chem.* **262**, 9412–9420 (1987).
6. H. Valadi *et al.*, "Exosome-mediated transfer of mRNAs and microRNAs is a novel mechanism of genetic exchange between cells," *Nat. Cell Biol.* **9**, 654–659 (2007).
7. M. Tkach, C. Thery, "Communication by extracellular vesicles: Where we are and where we need to go," *Cell* **164**, 1226–1232 (2016).
8. H. Liu, X. Sun, X. Gong, G. Wang, "Human umbilical cord mesenchymal stem cells derived exosomes exert antiapoptosis effect via activating PI3K/Akt/mTOR pathway on H9C2 cells," *J. Cell Biochem.* **120**, 14455–14464 (2019).
9. J. Zheng *et al.*, "Extracellular vesicles derived from human umbilical cord mesenchymal stem cells protect liver ischemia/reperfusion injury by reducing CD154 expression on CD4+ T cells via CCT2," *Adv. Sci. (Weinh)* **7**, 1903746 (2020).
10. M. Mathieu, L. Martin-Jaular, G. Lavieu, C. Thery, "Specificities of secretion and uptake of exosomes and other extracellular vesicles for cell-to-cell communication," *Nat. Cell Biol.* **21**, 9–17 (2019).

11. S. Keshtkar, N. Azarpira, M. H. Ghahremani, "Mesenchymal stem cell-derived extracellular vesicles: Novel frontiers in regenerative medicine," *Stem Cell. Res. Ther.* **9**, 63 (2018).
12. S. Koniusz *et al.*, "Extracellular vesicles in physiology, pathology, and therapy of the immune and central nervous system, with focus on extracellular vesicles derived from mesenchymal stem cells as therapeutic tools," *Front. Cell. Neurosci.* **10**, 109 (2016).
13. L. V. K. Reddy, D. Murugan, M. Mullick, E. T. Begum Moghal, D. Sen, "Recent approaches for angiogenesis in search of successful tissue engineering and regeneration," *Curr. Stem Cell Res. Ther.* **15**, 111–134 (2020).
14. S. Zhang *et al.*, "MSC exosomes mediate cartilage repair by enhancing proliferation, attenuating apoptosis and modulating immune reactivity," *Biomaterials* **156**, 16–27 (2018).
15. G. R. Willis *et al.*, "Mesenchymal stromal cell exosomes ameliorate experimental bronchopulmonary dysplasia and restore lung function through macrophage immunomodulation," *Am. J. Respir. Crit. Care Med.* **197**, 104–116 (2018).
16. G. Qiu *et al.*, "Mesenchymal stem cell-derived extracellular vesicles affect disease outcomes via transfer of microRNAs," *Stem Cell. Res. Ther.* **9**, 320 (2018).
17. J. Yao *et al.*, "Extracellular vesicles derived from human umbilical cord mesenchymal stem cells alleviate rat hepatic ischemia-reperfusion injury by suppressing oxidative stress and neutrophil inflammatory response," *FASEB J.* **33**, 1695–1710 (2019).
18. W. Jiang *et al.*, "Human umbilical cord MSC-derived exosomes suppress the development of CCl_4-induced liver injury through antioxidant effect," *Stem Cells Int.* **2018**, 6079642 (2018).
19. K. Xie, L. Liu, J. Chen, F. Liu, "Exosomes derived from human umbilical cord blood mesenchymal stem cells improve hepatic ischemia reperfusion injury via delivering miR-1246," *Cell Cycle* **18**, 3491–3501 (2019).
20. A. Ciullo *et al.*, "Exosomal expression of $CXCR_4$ targets cardioprotective vesicles to myocardial infarction and improves outcome after systemic administration," *Int. J. Mol. Sci.* **20**, 468 (2019).
21. S. Fujii *et al.*, "Graft-Versus-Host disease amelioration by human bone marrow mesenchymal stromal/stem cell-derived extracellular vesicles is associated with peripheral preservation of naive T cell populations," *Stem Cells* **36**, 434–445 (2018).
22. L. Kordelas *et al.*, "MSC-derived exosomes: A novel tool to treat therapy-refractory graft-versus-host disease," *Leukemia* **28**, 970–973 (2014).
23. H. Cao *et al.*, "*In vivo* tracking of mesenchymal stem cell-derived extracellular vesicles improving mitochondrial function in renal ischemia-reperfusion injury," *ACS Nano* **14**, 4014–4026 (2020).
24. Y. Chen, K. Xue, X. Zhang, Z. Zheng, K. Liu, "Exosomes derived from mature chondrocytes facilitate subcutaneous stable ectopic chondrogenesis of cartilage progenitor cells," *Stem Cell. Res. Ther.* **9**, 318 (2018).
25. B. You, W. Xu, B. Zhang, "Engineering exosomes: a new direction for anticancer treatment," *Am. J. Cancer Res.* **8**, 1332–1342 (2018).
26. A. Thakur *et al.*, "Inhibition of glioma cells' proliferation by doxorubicin-loaded exosomes via microfluidics," *Int. J. Nanomed.* **15**, 8331–8343 (2020).
27. S. K. Limoni, M. F. Moghadam, S. M. Moazzeni, H. Gomari, F. Salimi, "Engineered exosomes for targeted transfer of siRNA to HER_2 positive breast cancer cells," *Appl. Biochem. Biotechnol.* **187**, 352–364 (2019).
28. S. T. Chuo, J. C. Chien, C. P. Lai, "Imaging extracellular vesicles: Current and emerging methods," *J. Biomed. Sci.* **25**, 91 (2018).
29. V. Hyenne, O. Lefebvre, J. G. Goetz, "Going live with tumor exosomes and microvesicles," *Cell Adh. Migr.* **11**, 173–186 (2017).
30. Y.-J. Li, J.-Y. Wu, J.-M. Wang, X.-B. Hu, D.-X. Xiang, "Emerging strategies for labeling and tracking of extracellular vesicles," *J. Controlled Release* **328**, 141–159 (2020).
31. O. Betzer *et al.*, "Advances in imaging strategies for *in vivo* tracking of exosomes," *Wiley Interdiscip. Rev. Nanomed. Nanobiotechnol.* **12**, e1594 (2019).
32. O. P. Wiklander *et al.*, "Extracellular vesicle*in vivo* biodistribution is determined by cell source, route of administration and targeting," *J. Extracell. Vesicles* **4**, 26316 (2015).
33. S. Wen *et al.*, "Biodistribution of mesenchymal stem cell-derived extracellular vesicles in a radiation injury bone marrow murine model," *Int. J. Mol. Sci.* **20**, 5468 (2019).
34. S. W. Wen *et al.*, "The Biodistribution and immune suppressive effects of breast cancer-derived exosomes," *Cancer Res.* **76**, 6816–6827 (2016).
35. M. Mendt *et al.*, "Generation and testing of clinical-grade exosomes for pancreatic cancer," *JCI Insight* **3**, e99263 (2018).
36. R. Tamura, S. Uemoto, Y. Tabata, "Immunosuppressive effect of mesenchymal stem cell-derived exosomes on a concanavalin A-induced liver injury model," *Inflamm. Regen.* **36**, 26 (2016).
37. R. Tamura, S. Uemoto, Y. Tabata, "Augmented liver targeting of exosomes by surface modification with cationized pullulan," *Acta Biomater.* **57**, 274–284 (2017).

38. A. E. Russell *et al.*, "Biological membranes in EV biogenesis, stability, uptake, and cargo transfer: An ISEV position paper arising from the ISEV membranes and EVs workshop," *J. Extracell. Vesicles* **8**, 1684862 (2019).
39. P. Zhang *et al.*, "*In vivo* tracking of multiple tumor exosomes labeled by phospholipid-based bioorthogonal conjugation," *Anal. Chem.* **90**, 11273–11279 (2018).
40. S. M. Kim *et al.*, "Cancer-derived exosomes as a delivery platform of CRISPR/Cas9 confer cancer cell tropism-dependent targeting," *J. Control. Release* **266**, 8–16 (2017).
41. Z. Yang *et al.*, "Functional exosome-mimic for delivery of siRNA to cancer: *In vitro* and *in vivo* evaluation," *J. Control. Release* **243**, 160–171 (2016).
42. H. Cao *et al.*, "*In vivo* real-time imaging of extracellular vesicles in liver regeneration via aggregation-induced emission luminogens," *ACS Nano* **13**, 3522–3533 (2019).
43. A. Zomer *et al.*, "*In vivo* imaging reveals extracellular vesicle-mediated phenocopying of metastatic behavior," *Cell* **161**, 1046–1057 (2015).
44. A. Suetsugu *et al.*, "Imaging exosome transfer from breast cancer cells to stroma at metastatic sites in orthotopic nude-mouse models," *Adv. Drug Deliv. Rev.* **65**, 383–390 (2013).
45. C. P. Lai *et al.*, "Visualization and tracking of tumour extracellular vesicle delivery and RNA translation using multiplexed reporters," *Nat. Commun.* **6**, 7029 (2015).
46. S. Manca *et al.*, "Milk exosomes are bioavailable and distinct microRNA cargos have unique tissue distribution patterns," *Sci. Rep.* **8**, 11321 (2018).
47. C. E. Badr, B. A. Tannous, "Bioluminescence imaging: Progress and applications," *Trends Biotechnol.* **29**, 624–633 (2011).
48. Y. Takahashi *et al.*, "Visualization and *in vivo* tracking of the exosomes of murine melanoma B16-BL6 cells in mice after intravenous injection," *J. Biotechnol.* **165**, 77–84 (2013).
49. T. Imai *et al.*, "Macrophage-dependent clearance of systemically administered B16BL6-derived exosomes from the blood circulation in mice," *J. Extracell. Vesicles* **4**, 26238 (2015).
50. C. Charoenviriyakul *et al.*, "Cell type-specific and common characteristics of exosomes derived from mouse cell lines: Yield, physicochemical properties, and pharmacokinetics," *Eur. J. Pharm. Sci.* **96**, 316–322 (2017).
51. K. Zhang *et al.*, "Enhanced therapeutic effects of mesenchymal stem cell-derived exosomes with an injectable hydrogel for hindlimb ischemia treatment," *ACS Appl. Mater. Interf.* **10**, 30081–30091 (2018).
52. C. P. Lai *et al.*, "Dynamic biodistribution of extracellular vesicles *in vivo* using a multimodal imaging reporter," *ACS Nano* **8**, 483–494 (2014).
53. K. E. van der Vos *et al.*, "Directly visualized glioblastoma-derived extracellular vesicles transfer RNA to microglia/macrophages in the brain," *Neuro-Oncol.* **18**, 58–69 (2016).
54. T. Hikita, M. Miyata, R. Watanabe, C. Oneyama, "Sensitive and rapid quantification of exosomes by fusing luciferase to exosome marker proteins," *Sci. Rep.* **8**, 14035 (2018).
55. P. Gangadaran *et al.*, "A new bioluminescent reporter system to study the biodistribution of systematically injected tumor-derived bioluminescent extracellular vesicles in mice," *Oncotarget* **8**, 109894–109914 (2017).
56. B. C. Ahn, "Requisites for successful theranostics with radionuclide-based reporter gene imaging," *J. Drug Target.* **22**, 295–303 (2014).
57. M. H. Rashid *et al.*, "Differential *in vivo* biodistribution of ^{131}I-labeled exosomes from diverse cellular origins and its implication for theranostic application," *Nanomedicine* **21**, 102072 (2019).
58. M. Morishita *et al.*, "Quantitative analysis of tissue distribution of the B16BL6-derived exosomes using a streptavidin–lactadherin fusion protein and iodine-125-labeled biotin derivative after intravenous injection in mice," *J. Pharm. Sci.* **104**, 705–713 (2015).
59. T. Smyth *et al.*, "Biodistribution and delivery efficiency of unmodified tumor-derived exosomes," *J. Control. Release.* **199**, 145–155 (2015).
60. F. N. Faruqu *et al.*, "Membrane radiolabelling of exosomes for comparative biodistribution analysis in immunocompetent and immunodeficient mice — A novel and universal approach," *Theranostics* **9**, 1666–1682 (2019).
61. D. W. Hwang *et al.*, "Noninvasive imaging of radiolabeled exosome-mimetic nanovesicle using ^{99m}Tc-HMPAO," *Sci. Rep.* **5**, 15636 (2015).
62. Z. Varga *et al.*, "Radiolabeling of extracellular vesicles with ^{99m}Tc for quantitative *in vivo* imaging studies," *Cancer Biother. Radiopharm.* **31**, 168–173 (2016).
63. P. Gangadaran *et al.*, "*In vivo* non-invasive imaging of radio-labeled exosome-mimetics derived from red blood cells in mice," *Front. Pharmacol.* **9**, 817 (2018).
64. M. I. Gonzalez, P. Martin-Duque, M. Desco, B. Salinas, "Radioactive labeling of milk-derived exosomes with ^{99m}Tc and *in vivo* tracking by SPECT imaging," *Nanomaterials (Basel)* **10**, 1062 (2020).
65. S. Molavipordanjani *et al.*, "^{99m}Tc-radiolabeled HER_2 targeted exosome for tumor imaging," *Eur. J. Pharm. Sci.* **148**, 105312 (2020).

66. S. Shi *et al.*, "Copper-64 labeled PEGylated exosomes for *in vivo* positron emission tomography and enhanced tumor retention," *Bioconjug. Chem.* **30**, 2675–2683 (2019).
67. K. O. Jung *et al.*, "Identification of lymphatic and hematogenous routes of rapidly labeled radioactive and fluorescent exosomes through highly sensitive multimodal imaging," *Int. J. Mol. Sci.* **21**, 7850 (2020).
68. F. Royo, U. Cossio, A. Ruiz de Angulo, J. Llop, J. M. Falcon-Perez, "Modification of the glycosylation of extracellular vesicles alters their biodistribution in mice," *Nanoscale* **11**, 1531–1537 (2019).
69. O. Betzer *et al.*, "*In vivo* neuroimaging of exosomes using gold nanoparticles," *ACS Nano* **11**, 10883–10893 (2017).
70. S. Guo *et al.*, "Intranasal delivery of mesenchymal stem cell derived exosomes loaded with phosphatase and tensin homolog siRNA repairs complete spinal cord injury," *ACS Nano* **13**, 10015–10028 (2019).
71. N. Perets *et al.*, "Golden exosomes selectively target brain pathologies in neurodegenerative and neurodevelopmental disorders," *Nano Lett.* **19**, 3422–3431 (2019).
72. P. Lara *et al.*, "Gold nanoparticle based double-labeling of melanoma extracellular vesicles to determine the specificity of uptake by cells and preferential accumulation in small metastatic lung tumors," *J. Nanobiotechnol.* **18**, 20 (2020).
73. L. Hu, S. A. Wickline, J. L. Hood, "Magnetic resonance imaging of melanoma exosomes in lymph nodes," *Magn. Reson. Med.* **74**, 266–271 (2015).
74. K. O. Jung, H. Jo, J. H. Yu, S. S. Gambhir, G. Pratx, "Development and MPI tracking of novel hypoxia-targeted theranostic exosomes," *Biomaterials* **177**, 139–148 (2018).
75. A. Busato *et al.*, "Magnetic resonance imaging of ultrasmall superparamagnetic iron oxide-labeled exosomes from stem cells: A new method to obtain labeled exosomes," *Int. J. Nanomed.* **11**, 2481–2490 (2016).
76. A. Busato *et al.*, "Labeling and magnetic resonance imaging of exosomes isolated from adipose stem cells," *Curr. Protoc. Cell Biol.* **75**, 3. 44. 1–3. 44. 15 (2017).
77. J. Abello, T. D. T. Nguyen, R. Marasini, S. Aryal, M. L. Weiss, "Biodistribution of gadolinium- and near infrared-labeled human umbilical cord mesenchymal stromal cell-derived exosomes in tumor bearing mice," *Theranostics* **9**, 2325–2345 (2019).
78. R. J. C. Bose *et al.*, "Tumor cell-derived extracellular vesicle-coated nanocarriers: An efficient theranostic platform for the cancer-specific delivery of anti-miR-21 and imaging agents," *ACS Nano* **12**, 10817–10832 (2018).
79. T. Liu, Y. Zhu, R. Zhao, X. Wei, X. Xin, "Visualization of exosomes from mesenchymal stem cells *in vivo* by magnetic resonance imaging," *Magn. Reson. Imag.* **68**, 75–82 (2020).
80. C. Kim, C. Favazza, L. V. Wang, "*In vivo* photoacoustic tomography of chemicals: High-resolution functional and molecular optical imaging at new depths," *Chem. Rev.* **110**, 2756–2782 (2010).
81. Q. Chen *et al.*, "A self-assembled albumin-based nanoprobe for *in vivo* ratiometric photoacoustic pH imaging," *Adv. Mater.* **27**, 6820–6827 (2015).
82. Y. Li, Y. Chen, M. Du, Z.-Y. Chen, "Ultrasound technology for molecular imaging: From contrast agents to multimodal imaging," *ACS Biomater Sci. Eng.* **4**, 2716–2728 (2018).
83. Q. Chen *et al.*, "H_2O_2-responsive liposomal nanoprobe for photoacoustic inflammation imaging and tumor theranostics via in vivo chromogenic assay," *Proc. Natl. Acad. Sci/USA.* **114**, 5343–5348 (2017).
84. Y. J. Piao *et al.*, "Breast cancer cell-derived exosomes and macrophage polarization are associated with lymph node metastasis," *Oncotarget* **9**, 7398–7410 (2018).
85. H. Ding *et al.*, "Exosome-like nanozyme vesicles for H_2O_2-responsive catalytic photoacoustic imaging of xenograft nasopharyngeal carcinoma," *Nano Lett.* **19**, 203–209 (2019).
86. Y. Jang *et al.*, "Exosome-based photoacoustic imaging guided photodynamic and immunotherapy for the treatment of pancreatic cancer," *J. Control. Release.* **330**, 293–304 (2020).
87. D. Zhu *et al.*, "Stellate plasmonic exosomes for penetrative targeting tumor NIR-II thermo-radiotherapy," *ACS Appl. Mater. Interfaces* **12**, 36928–36937 (2020).
88. J. Y. Zhao *et al.*, "Ultrasmall magnetically engineered Ag_2Se quantum dots for instant efficient labeling and whole-body high-resolution multimodal real-time tracking of cell-derived microvesicles," *J. Am. Chem. Soc.* **138**, 1893–1903 (2016).
89. Y. Cao *et al.*, "Engineered exosome-mediated near-infrared-II region V_2C quantum dot delivery for nucleus-target low-temperature photothermal therapy," *ACS Nano* **13**, 1499–1510 (2019).
90. S. Shaikh *et al.*, "Real-time multimodal bioimaging of cancer cells and exosomes through biosynthesized iridium and iron nanoclusters," *ACS Appl. Mater. Interfaces.* **10**, 26056–26063 (2018).